An Autophagy-Independent Role for *ATG41* in Sulfur Metabolism During Zinc Deficiency

Michael D. Bucci,* Erin Weisenhorn,† Spencer Haws,* Zhiyuan Yao,‡ Ginelle Zimmerman,* Molly Gannon,* Janet Taggart,* Traci Lee,§ Daniel J. Klionsky,‡ Jason Russell,,†† Joshua Coon,†,**,††,‡‡ and David J. Eide*,1**

*Department of Nutritional Sciences, †Department of Biomolecular Chemistry, ††Genome Center of Wisconsin, and ‡‡Department of Chemistry, University of Wisconsin–Madison, Wisconsin 53706, ‡Department of Molecular, Cellular and Developmental Biology, Life Sciences Institute, University of Michigan, Ann Arbor, Michigan 48109, §Department of Biological Sciences, University of Wisconsin–Parkside, Kenosha, Wisconsin 53144, and **Morgridge Institute for Research, Madison, Wisconsin 53715

ABSTRACT The Zap1 transcription factor of *Saccharomyces cerevisiae* is a key regulator in the genomic responses to zinc deficiency. Among the genes regulated by Zap1 during zinc deficiency is the autophagy-related gene *ATG41*. Here, we report that Atg41 is required for growth in zinc-deficient conditions, but not when zinc is abundant or when other metals are limiting. Consistent with a role for Atg41 in macroautophagy, we show that nutritional zinc deficiency induces autophagy and that mutation of *ATG41* diminishes that response. Several experiments indicated that the importance of *ATG41* function to growth during zinc deficiency is not because of its role in macroautophagy, but rather is due to one or more autophagy-independent functions. For example, rapamycin treatment fully induced autophagy in zinc-deficient *atg41*Δ mutants but failed to improve growth. In addition, *atg41*Δ mutants showed a far more severe growth defect than any of several other autophagy mutants tested, and *atg41*Δ mutants showed increased Heat Shock Factor 1 activity, an indicator of protein homeostasis stress, while other autophagy mutants did not. An autophagy-independent function for *ATG41* in sulfur metabolism during zinc deficiency was suggested by analyzing the transcriptome of *atg41*Δ mutants during the transition from zinc-replete to -deficient conditions. Analysis of sulfur metabolites confirmed that Atg41 is needed for the normal accumulation of methionine, homocysteine, and cysteine in zinc-deficient cells. Therefore, we conclude that Atg41 plays roles in both macroautophagy and sulfur metabolism during zinc deficiency.

KEYWORDS autophagy; zinc deficiency; sulfur metabolism; yeast; *Saccharomyces cerevisiae*

ZINC plays structural and catalytic roles for a large number of proteins. This metal nutrient is also toxic if overaccumulated, so mechanisms of zinc homeostasis are essential. The Zap1 transcription factor is the master regulator of zinc homeostasis in the yeast *Saccharomyces cerevisiae*. The primary function of this protein is to activate the expression of specific target genes in response to zinc deficiency. Approximately 80 Zap1-regulated genes have been previously identified. Among these target genes are those encoding the plasma membrane zinc transporters Zrt1, Zrt2, and Fet4, which are responsible for zinc uptake into the cell and organellar transporters that maintain zinc levels within cellular compartments (*e.g.*, Zrg17 and Zrc1) or mobilize organellar zinc stores (*e.g.*, Zrt3) (Lyons *et al.* 2000; Han *et al.* 2005; De Nicola *et al.* 2007; Wu *et al.* 2008, 2009; Soto-Cardalda *et al.* 2012; Singh *et al.* 2016). These proteins serve to maintain zinc homeostasis over a wide range of extracellular zinc availability. Zap1 also regulates genes involved in adapting cellular processes to the challenges of zinc deficiency. For example, the *CKI1* and *EKI1* genes are induced by Zap1 to maintain phospholipid synthesis (Kersting and Carman 2006; Soto and Carman 2008). The *CTT1* catalase gene is also induced by Zap1 and this response is likely to eliminate the oxidative stress that arises during zinc deficiency. The protein chaperones Hsp26 and Tsa1 are induced to deal with unfolded protein stress that might occur due to a lack of this important structural cofactor, and *UBI4*, encoding ubiquitin, is activated by Zap1 to maintain levels of this critical stress

doi: https://doi.org/10.1534/genetics.117.300679
Manuscript received October 9, 2017; accepted for publication January 5, 2018; published Early Online January 10, 2018.
Supplemental material is available online at www.genetics.org/lookup/suppl/doi:10.1534/genetics.117.300679/-/DC1.
[1]Corresponding author: Department of Nutritional Sciences, University of Wisconsin–Madison, 1415 Linden Dr., Madison, WI 53706. E-mail: deide@wisc.edu

protein (MacDiarmid *et al.* 2013, 2016). Thus, Zap1 plays important roles in maintaining zinc homeostasis and adapting the cell to zinc-deficient growth.

Another Zap1 target gene induced by zinc deficiency is *ATG41*, which was previously known as *ICY2*. The first reports of *ATG41* function were related to a possible role in protein homeostasis. Mutation of *ATG41* further impaired growth of a strain with a temperature-sensitive mutation in the *TCP1* chaperonin α subunit gene (D. Ursic, *Saccharomyces* Genome Database). The chaperonin complex mediates folding of many proteins in the cytosol (Spiess *et al.* 2004). Overexpression of *ATG41* was also found to suppress the growth-inhibitory effects of SNCA/α-synuclein expression in yeast (Yeger-Lotem *et al.* 2009). The SNCA protein is involved in the pathology of Parkinson's disease and its expression in yeast results in many perturbations of cellular systems, including the formation of cytosolic protein aggregates (Outeiro and Lindquist 2003). Also consistent with a role in protein homeostasis, *ATG41* was identified as being activated by the Heat Shock Factor 1 (Hsf1) heat shock response factor during heat shock (Hahn *et al.* 2004).

More recently, *ATG41* was shown to be induced by the Gcn4 transcription factor and to be required for macroautophagy in nitrogen-starved cells (Yao *et al.* 2015). Macroautophagy (hereafter referred to as autophagy) is a process in which the cell forms a double-membrane vesicle called the autophagosome around regions of cytoplasm, and then delivers it to the lysosome or vacuole for degradation and recycling (Yin *et al.* 2016). Autophagy is canonically induced by nitrogen starvation conditions, but it is also induced by carbon source restriction and by methionine starvation (Stephan *et al.* 2009; Wu and Tu 2011; Sutter *et al.* 2013). Approximately 20 proteins are known to be required for formation and degradation of autophagosomes by autophagy, with many of these localizing to the phagophore assembly site where vesicle formation around the cargo occurs (Suzuki *et al.* 2007). The process of nonselective autophagy contrasts with various types of cargo-selective autophagy-related processes. Whereas autophagy can be nonspecific for the sequestered cargo, processes such as mitophagy and pexophagy are specific for mitochondria and peroxisomes, respectively (Kraft *et al.* 2009).

Our previous study using functional profiling of the yeast deletion collection suggested that the process of autophagy is important for zinc-deficient growth (North *et al.* 2012). Several mutants disrupted for autophagy function show mild but detectable growth defects in zinc-deficient conditions. Carman and colleagues presented the first evidence we are aware of that autophagy is induced by zinc deficiency. They observed that lipidation of the Atg8 autophagy factor, an event that occurs during autophagy, is increased in zinc-deficient cells (Iwanyshyn *et al.* 2004). More recently, Ohsumi and colleagues showed that the process of autophagy is induced when intracellular zinc levels are perturbed by treatment with a cell-permeable metal chelator (Kawamata *et al.* 2017). This chelator-induced process is regulated by the target of rapamycin complex 1 (TORC1) and is Zap1-independent.

In this report, we examined the function of the *ATG41* gene during zinc deficiency. Relative to other Zap1 target genes, we found that *ATG41* is among the most critical for growth under these conditions. We confirmed that autophagy is induced by nutritional zinc deficiency and that this process is defective in *atg41*Δ mutants. However, we present several lines of evidence that the critical role of *ATG41* during zinc deficiency is likely to be unrelated to its function in autophagy. Consistent with this protein having other functions, we discovered that Atg41 is required for normal sulfur metabolism in zinc-deficient cells. Thus, our results demonstrate that Atg41 plays autophagy-dependent and -independent roles when zinc is limiting.

Materials and Methods

Strains and media

Strains used are listed in Supplemental Material, Table S1 in File S1. Cells were cultured in YPD (1% yeast extract, 2% peptone, and 2% glucose) or yeast nitrogen base plus 0.01% of auxotrophic supplements and 2% glucose. Limited zinc medium (LZM) was prepared as described previously (Zhao and Eide 1996) and supplemented for optimal growth of S288C-derived strains (Hanscho *et al.* 2012). LZM was supplemented with either 1 or 100 μM $ZnCl_2$ for zinc-deficient or zinc-replete conditions, respectively. Methionine (0.01%) was added unless indicated otherwise. For iron- or copper-limiting medium, LZM was supplemented with 100 μM $ZnCl_2$ and the indicated concentration of the metal in question. For batch culture experiments, statistical significance was assessed using Student's *t*-test. Strains used were of the S288C background and derived from BY4743, BY4741, or BY4742. The DY1457 *atg41*Δ strain (W303 background) was generated by transforming (Gietz *et al.* 1992) a PCR product containing the G418 resistance cassette (KanMX4) targeted to delete the *ATG41* open reading frame (ORF) by homologous recombination. MDB01 and MDB02 were obtained by sporulation and tetrad dissection of BY4743 *atg41*Δ.

Plasmids

pATG41 was made by inserting an *ATG41* gene clone into pRS313 (77142; ATCC). This plasmid contains 1000 bp upstream and 500 bp downstream of the *ATG41* ORF. pICY1-OE was constructed by cloning the *ICY1* ORF into the pDR195 (36028; Addgene) multiple cloning site using homologous recombination. This plasmid contains 1000 bp upstream and 500 bp downstream of the *ICY1* ORF. The *SSA3*-LacZ reporter (pSSA3-LacZ) was obtained from the laboratory of Dennis Thiele (Duke University School of Medicine). pGFP-Atg8 and pHSE-LacZ were described previously (Suzuki *et al.* 2001; MacDiarmid *et al.* 2016).

Reporter assays

Experiments with the pSSA3-LacZ reporter were conducted using ortho-nitrophenyl-β-galactoside (Guarente 1983), with cells grown to midlog phase in either zinc-replete or zinc-deficient

LZM. Assays using the pHSE-LacZ reporter were conducted using the β-Glo Assay System (Promega, Madison, WI). Aliquots of cultures were diluted to an OD_{600} of 0.1. Fifteen microliters of diluted cells were mixed with an equal volume of the β-Glo reagent in a clear 1.5-ml microcentrifuge tube. After incubating at room temperature for 30 min, luminescence was measured using a GloMax 20/20 Single-Tube Luminometer.

Competitive growth assays

Growth assays of deletion mutants *vs.* wild-type cells were carried out as previously described (MacDiarmid *et al.* 2016). Wild-type cells expressing GFP and untagged mutants were grown separately in liquid culture, mixed in equal numbers, and grown for 15 generations in zinc-replete or -deficient media. After analysis by flow cytometry on a FACSCalibur flow cytometer (BD Biosciences), the final percentages of mutant cells in each culture were determined. To calculate a fitness ratio, we averaged the percent of mutant cells remaining after 15 generations in three independent replicates for both zinc-deficient and -replete conditions. The percent of mutant cells remaining after zinc-deficient growth was then divided by the percent of mutant cells after replete growth. A ratio below one indicated a zinc-limited growth defect. Statistical significance was determined by Student's *t*-test after Benjamini–Hochberg correction. Control experiments demonstrated that untagged and GFP-expressing wild-type cells show no difference in growth (fitness ratio = 1) in this assay (MacDiarmid *et al.* 2016).

Autophagy assays

For GFP-Atg8 processing assays, cultures were grown overnight to saturation, then inoculated into LZM plus 100 μM $ZnCl_2$ and allowed to reach log-phase growth overnight. Samples for immunoblotting were taken from the zinc-replete cultures, and the remaining cells were washed and transferred to the zinc-deficient medium for 8 hr before collection for immunoblotting. For the precursor Ape1 (prApe1) processing assay, cells were treated identically, except they were grown in the zinc-deficient medium for 4 hr.

Immunoblotting

Cell pellets were processed using trichloroacetic acid as previously described to produce total protein extracts (MacDiarmid *et al.* 2013). SDS-PAGE, immunoblotting, and imaging were also performed as previously described (MacDiarmid *et al.* 2013). The anti-GFP antibody was obtained from Roche (11814460001) and the anti-Pgk1 antibody from Abcam (22C5D8). Band intensities were quantified using the Image Studio software available from LI-COR Biosciences. Statistical significance of band intensities was assessed using the Student's *t*-test.

RNA sequencing (RNA-seq) analysis

Wild-type (BY4743), *atg1*Δ, and *atg41*Δ cells were grown to midlog phase in zinc-replete medium. Aliquots were then collected into a one-eighth volume of 5% phenol–95% ethanol. Cell pellets were collected in microcentrifuge tubes, frozen in liquid N_2, and stored at −80°. The remaining cells were washed three times in prewarmed zinc-deficient medium and inoculated into fresh zinc-deficient medium (triplicate cultures). Samples were collected identically to the zinc-replete samples after 8 hr. RNA quality control, library preparation, and sequencing were performed at the University of Wisconsin–Madison Biotechnology Center. mRNA was purified from 1 μg total RNA using poly(T) oligo-attached magnetic beads, and each RNA library was generated following the Illumina TruSeq RNA Sample Preparation v2 (Rev. E) Guide using the Illumina TruSeq RNA Sample Preparation Kit (Illumina, San Diego, CA). Quality and quantity of finished libraries were assessed using an Agilent DNA1000 series chip assay (Agilent Technologies) and a Qubit HS Kit (Invitrogen, Carlsbad, CA), respectively. Each library was standardized to 2 nM. Cluster generation was performed using a TruSeq Single-Read Cluster Kit (v4) and the Illumina cBot. Single-end, 100-bp sequencing was performed, using v4 sequencing by synthesis (SBS) chemistry on an Illumina HiSeq2500 sequencer. Images were analyzed using the standard Illumina Pipeline, version 1.8.2. Sequencing reads were adapter- and quality-trimmed to Q20 using the Skewer trimming program (Jiang *et al.* 2014). Alignment of sequence reads, clone sequences, and assembly contigs was performed with BWA-MEM (https://arxiv.org.abs/1303.3997v1). Quality reads were subsequently aligned to the annotated reference genome using the Spliced Transcripts Alignment to a Reference (STAR) aligner (Dobin *et al.* 2013). Quantification of expression for each gene was calculated by RNA-Seq by Expectation Maximization (RSEM) (Li and Dewey 2011). The expected read counts from RSEM were filtered for low/empty values, requiring at least 1 count per million in at least three samples. Differential gene expression analysis was performed using EdgeR (Robinson *et al.* 2010).

Quantitative RT-PCR analysis

RNA extraction and quantitative RT-PCR were performed according to previously described methods (MacDiarmid *et al.* 2016). In addition to previously described primers for the *18S* rRNA, *TAF10*, and *ACT1* (MacDiarmid *et al.* 2016), we used the following primer pairs: for *MET5*, 5′-CCCAAGATTAGGGTCATGCT-3′ and 5′-TTAAACGAGCATGCTTACGG-3′; for *SAM2*, 5′-GAAATTTCCACCGCTGACTT-3′ and 5′-GACCACCGATGACGAATCTA-3′; and for *SUL1*, 5′-AACTGCCAAAGTCATTGCTG-3′ and 5′-ACAATCCCACAAAGCAAACA-3′. Target gene expression was calculated relative to the average C_t values for the three control genes (*18S* rRNA, *TAF10*, and *ACT1*) selected from multiple candidate genes tested for their highly stable expression under the conditions used in our experiments (data not shown).

Elemental analysis

Wild-type (BY4743) and isogenic *atg41* cells were grown to midlog phase in zinc-replete medium. Aliquots were then washed three times in cold water, pelleted, and frozen in liquid nitrogen. The remaining cells were washed three times in prewarmed zinc-deficient medium and inoculated into fresh zinc-deficient medium. Samples were collected identically to the zinc-replete samples after 4, 8, 12, and 16 hr of

culturing. Total zinc, sulfur, magnesium, potassium, and phosphorous content was determined using inductively coupled plasma atomic emission spectrometry (ICP-AES). Cell pellets were desiccated by incubation at 60° for 12–18 hr and subsequent dry weights recorded. The dried yeast pellets were acid digested in 250 μl OmniTrace 70% HNO_3 (EMD Chemicals) at 60° for 12–18 hr with 150–200 rpm orbital shaking. The acid lysates were then diluted to 5% HNO_3 with OmniTrace water (EMD Chemicals) and analyzed by ICP-AES (5100 SVDV; Agilent Technologies). The ICP-AES was calibrated using National Institute of Standards and Technology (NIST)-traceable elemental standards and validated using NIST-traceable 1577b bovine liver reference material. The detection range for zinc was 0.005–5 ppm with interassay precision $<$ 10%. Cesium (50 ppm) was used for ionization suppression and yttrium (5 ppm) was used as an internal standard for all samples. The detection range for sulfur was 0.05–50 ppm with interassay precision $<$ 20%. All reagents and plasticware were certified or routinely tested for trace metal work. Zinc content was determined using native software (ICPExpert) and normalized to the dry weight of each sample.

Sulfur metabolite analysis

Wild-type (BY4743) and isogenic *atg41*Δ cells were grown to midlog phase in zinc-replete medium. Aliquots were collected as cell pellets in microcentrifuge tubes, frozen in liquid N_2, and stored at −80°. The remaining cultures were washed three times in prewarmed zinc-deficient medium and inoculated into fresh zinc-deficient medium. Samples were collected identically to the zinc-replete samples at 4, 8, and 12 hr of culturing. Frozen cell pellets were lysed in 300 μl cold methanol. Samples were then vortexed for 5 min and incubated at 4° for 10 min to extract metabolites. Proteins and metabolites were separated by centrifugation for 10 min at 13,400 × *g* and 4°. For analysis, 75 μl of metabolite-containing extract was combined with 25 μl dilution buffer (60% acetonitrile and 1 mM tris(2-carboxyethyl) phosphate (TCEP)), and 2 μl internal standard [5 μM ^{15}N methionine and 1 μM ^{15}N S-adenosyl methionine (SAM)]. In addition, standard curves for each metabolite were prepared with equivalent addition of internal standard.

Targeted LC-MS/MS experiments were performed using a TSQ Quantiva Triple Quadrupole mass spectrometer and UltiMate 3000 Rapid Separation Binary Pump (Thermo Fisher Scientific). Analytes were injected and separated on an ACQUITY BEH amide column (2.1 mm × 150 mm, 1.7 μm particle diameter; Waters Associates, Milford, MA) heated to 35°. Mobile phase A consisted of 10 mM ammonium formate with 0.1% formic acid, and mobile phase B was 95% acetonitrile with 10 mM ammonium formate and 0.1% formic acid. An 11-min gradient starting with 95% B and ending with 40% B was employed, with an 18-min total method runtime. Selected reaction monitoring scans were taken of selected metabolites using 2–3 transitions per metabolite and previously optimized transitions for each target. The total cycle time was 1 sec. The mass spectrometer was equipped with a heated electrospray ionization source operated in positive mode using a spray voltage of 3500 V. Sheath, auxiliary, and sweep gases were held at 25, 13, and 1 arbitrary units, respectively. The ion transfer tube was heated to 342° and the vaporizer temperature was set to 358°. Q1 and Q3 resolution were set to 0.7 and 2 full width at half maximum. Collision-induced association (CID) gas was set to 1.5 mTorr and 16 V was used for the source fragmentation parameter. The resulting LC-MS/MS data were processed using TraceFinder software version 4.0 (Thermo Fisher Scientific) and peak detection was manually confirmed. Metabolite peak areas were normalized using internal standards, corrected for total protein content, and metabolites were quantified with standard curves. Concentrations of all metabolites analyzed were above their respective detection limits and within the linear range of these standards.

Data availability

Strains and plasmids generated in this study are available upon request. Gene expression data are available at the Gene expression Omnibus under accession number GSE108603. Figures S1 and S2 in File S1 address the zinc-deficient growth phenotype of *atg41*Δ mutants. Figures S3 and S4 in File S1 show the response of *atg41*Δ mutants to sulfate and sulfur-containing metabolites. Table S1 in File S1 describes the strains used, Table S2 in File S1 reports the competitive growth analysis of Zap1 target genes, Tables S3 and S4 in File S1 report RNA-seq results, and Tables S5–S7 in File S1 report the Gene Ontology (GO) analysis of *atg41*Δ-specific mutant effects.

Results

Mutations in Zap1 target genes cause a range of growth phenotypes during zinc deficiency

We and others have previously identified ∼80 genes likely to be transcriptionally activated by Zap1 during zinc deficiency. Notably, only a few of these putative Zap1-regulated genes were identified as required for optimal zinc-deficient growth in a study using functional profiling of the yeast deletion collection (North *et al.* 2012). It was possible that the previous method used, *i.e.*, microarray analysis of PCR-amplified strain-specific "barcodes," was not sensitive enough to detect mild growth defects. To more precisely assess the importance of Zap1-regulated genes to zinc-deficient growth, we used the more sensitive method of pair-wise competitive growth assays combined with flow cytometry analysis. Briefly, equal numbers of wild-type cells expressing GFP and mutant cells expressing no GFP were mixed and inoculated into a zinc-deficient (LZM plus 1 μM $ZnCl_2$) medium. These mixed cultures were grown for 15 generations and then assayed by flow cytometry. If the mutant lagged behind the wild-type strain due to a zinc-deficient growth defect, a smaller percentage of untagged cells was detected in the population. To control for strains that grew poorly regardless of zinc status, we also performed the growth assay under zinc-replete conditions

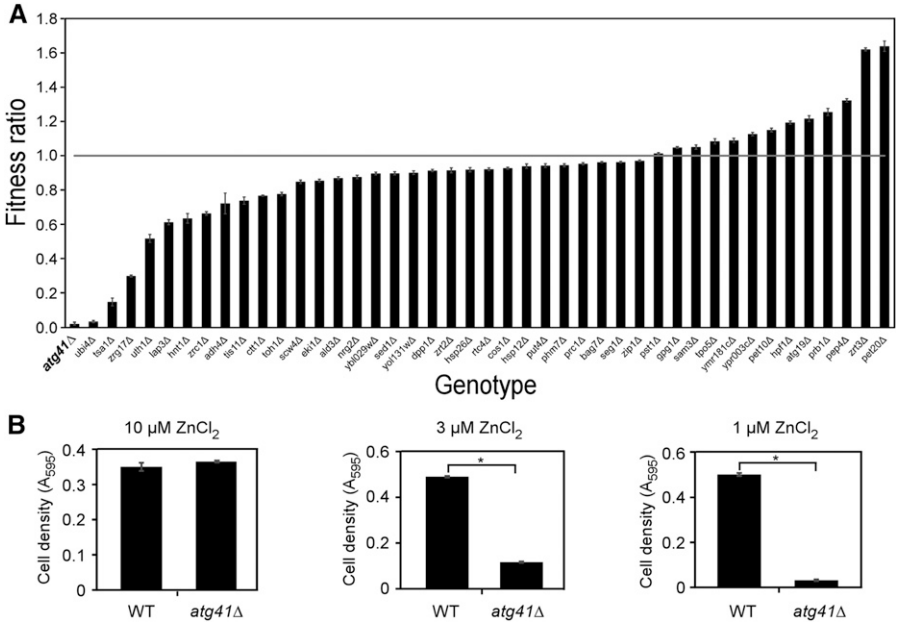

Figure 1 Growth analysis of Zap1-regulated genes. (A) Equal numbers of wild-type (WT) cells expressing GFP and untagged mutant cells were mixed in either zinc-replete or zinc-deficient medium. After growth for 15 generations, cultures were analyzed by FACS and cells were identified as either mutant or WT. The average percent mutant in zinc-deficient cultures was divided by the average percent mutant in zinc-replete cultures to obtain the fitness ratio values displayed. For all strains shown, the difference between average percent mutant in zinc-replete and -deficient cultures was significant ($P < 0.05$ by Student's *t*-test after Benjamini–Hochberg correction). Mutants showing no significant effect were not included. The line indicates a ratio of 1.0. (B) WT BY4743 or *atg41*Δ cells were grown in limited zinc medium supplemented with the indicated concentration of zinc chloride. For all panels, cultures were grown in triplicate and error bars represent 1 SD. The asterisks denote $P < 0.005$ by Students *t*-test.

(LZM plus 100 μM $ZnCl_2$). The full results of this analysis are reported in Table S2 in File S1.

The percentage of mutant cells remaining after growth in both zinc conditions was used to generate a fitness ratio of percent mutant after zinc-deficient growth divided by the percent mutant after zinc-replete growth (Figure 1A). A fitness ratio < 1.0 indicated a zinc-deficient growth defect for the corresponding mutant. The previous functional profiling study found only seven putative Zap1 targets that were required for efficient zinc-deficient growth (*ATG41*, *UBI4*, *TSA1*, *ZRG17*, *UTH1*, *HNT1*, and *ADH4*). However, using this more sensitive assay, we found that 31 of the 66 mutants tested showed a greater defect in zinc-deficient growth than zinc-replete growth. Many of these zinc-limited growth defects were mild, which is consistent with them being previously undetected. Notably, neither *ZRT1* nor *ZAP1* itself were assayed in this or the previous study because mutations in these critical genes fail to grow even under the replete conditions used; much higher concentrations of zinc are required to restore their growth. Relative to zinc-replete and -deficient wild-type cells, 14 mutants did not grow differently under either zinc condition ($P > 0.05$). Surprisingly, 13 mutants grew better than wild-type cells in zinc-deficient medium. The remaining eight mutants displayed more complex phenotypes (Table S2 in File S1). For example, *izh1*Δ, *ade17*Δ, *fet4*Δ, *moh1*Δ, and *vel1*Δ mutants had no low-zinc growth defect but a growth advantage in zinc-replete conditions. Therefore, these mutants had no growth defect in zinc deficiency despite having a fitness ratio < 1.0.

This analysis has provided a comprehensive assessment of the relative importance of putative Zap1-regulated genes to growth under zinc-deficient conditions. Among the mutants most severely defective for growth were *ubi4*Δ and *tsa1*Δ. *UBI4* encodes ubiquitin, and *TSA1* encodes a dual-function peroxidase and chaperone protein (MacDiarmid *et al.* 2013). For Tsa1, it was previously shown that the chaperone function is the more important for growth in limiting zinc (MacDiarmid *et al.* 2013). *UBI4* and *TSA1* are good examples of stress proteins regulated by Zap1 to allow cells to adapt to zinc deficiency. Of similar or even greater importance to zinc-deficient growth is the *ATG41* gene. This gene, which was previously known as *ICY2*, was recently shown to be important for efficient autophagy in response to nitrogen starvation (Yao *et al.* 2015).

Some Zap1-regulated genes, such as *UBI4*, are required for optimal growth under only the most severe conditions of zinc deficiency, whereas other genes (*e.g.*, *ZRT1*) are needed even under mild limitation. To further characterize *ATG41*'s importance during zinc deficiency, we performed growth experiments in LZM supplemented with 1–100 μM $ZnCl_2$. No growth defect was detected in LZM supplemented with zinc concentrations ranging from 10 to 100 μM $ZnCl_2$ (Figure 1B and data not shown). However, growth of the *atg41*Δ strain was significantly decreased in medium supplemented with either 1 or 3 μM $ZnCl_2$, *i.e.*, conditions of severe zinc limitation in this metal-buffered medium. We verified that the growth defect was due to the *atg41*Δ mutation; a wild-type *ATG41* plasmid fully complemented the defect (Figure S1 in File S1). We also determined that the growth defect of *atg41*Δ mutants was specific to zinc deficiency and was not observed under conditions of copper or iron deficiency (Figure S2 in File S1). These data indicated that the *ATG41* gene is needed specifically under severe, but not mild, zinc deficiency.

ATG41 and its paralog ICY1 share overlapping functions

The yeast genome contains a paralog to the *ATG41* gene called *ICY1*. Both genes encode short (~130 amino acid) proteins that are highly acidic with isoelectric points of ~4.0 (Figure 2A). To assess the role of Icy1 during zinc deficiency, competitive growth experiments were performed as described for

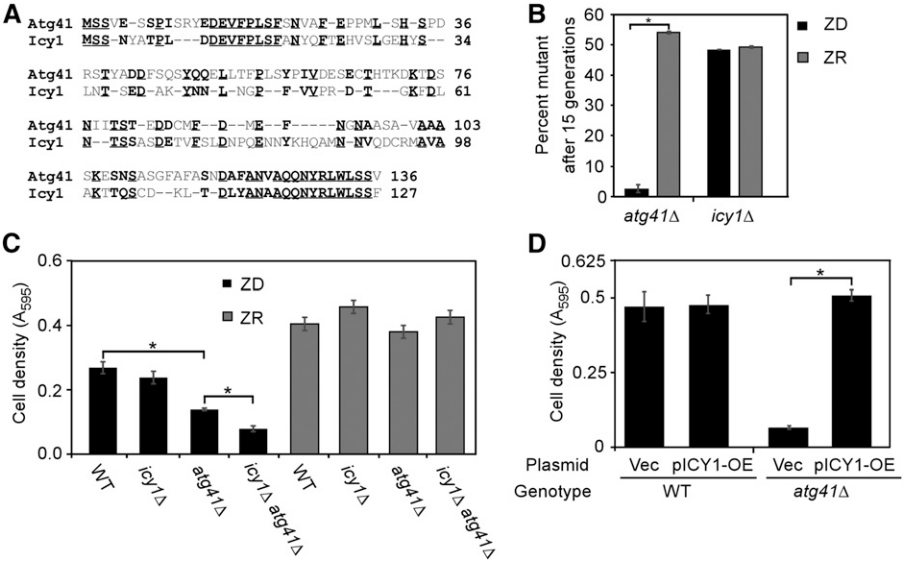

Figure 2 Atg41 and Icy1 have overlapping functions. (A) Amino acid sequence alignment of Atg41 and Icy1. Sites of identity are bold and underlined, sites of similarity are bold. (B) GFP-expressing wild-type (WT) cells were mixed in equal number with either *atg41*Δ or *icy1*Δ cells and grown in either zinc-replete (ZR) or zinc-deficient (ZD) medium. Subsequently, the percentage of mutant cells remaining in the cultures after 15 generations of growth was measured by FACS. The fitness ratio for the *atg41*Δ mutant calculated from these data were 0.049, and the fitness ratio for the *icy1*Δ mutant was 0.983. (C) WT, *icy1*Δ, *atg41*Δ, and *icy1*Δ *atg41*Δ cells were grown in ZR or ZD media. (D) WT and *atg41*Δ cells were transformed with either empty vector or pICY1-OE, and grown in ZD medium. For all panels, cultures were assayed in triplicate and error bars represent 1 SD. The asterisks denote $P < 0.05$ by Students *t*-test.

Figure 1A. Both *atg41*Δ and *icy1*Δ single mutants grew well relative to wild-type cells in zinc-replete conditions (Figure 2B). Under zinc deficiency, *atg41*Δ cells showed the expected strong growth defect while *icy1*Δ mutants were not significantly affected. To determine if a smaller contribution by Icy1 was being masked by Atg41 activity, the *ICY1* gene was deleted in an *atg41*Δ strain, and assessed for zinc-replete and -deficient growth in batch cultures. Mutation of *ICY1* in an *atg41*Δ strain caused decreased fitness in zinc-deficient cells, suggesting that Icy1 does contribute to an *ATG41*-dependent function (Figure 2C). No defect was seen for the double mutant in zinc-replete conditions. As an additional test of overlapping Atg41 and Icy1 function, we overexpressed the *ICY1* gene from the strong *PMA1* promoter in wild-type and *atg41*Δ mutant cells. While overexpression of *ICY1* had no effect on zinc-deficient growth of wild-type cells, growth of the *atg41*Δ strain was completely restored by Icy1 overexpression (Figure 2D). These results indicate that Icy1 contributes to Atg41's function during zinc deficiency. Previous studies showed that Atg41 was required for autophagy in response to nitrogen starvation but that Icy1 was not. These new data indicate that Icy1 does contribute to Atg41's critical function in zinc-deficient cells. Given that the single *icy1*Δ mutation has little phenotypic effect, we conclude that Atg41 plays the major role.

ATG41 is required for efficient autophagy that is induced by zinc deficiency

When autophagy is induced in response to nitrogen starvation, Atg41 is needed for maximal flux through the autophagic pathway (Yao *et al.* 2015). Considering our previous observation that autophagy is required for efficient zinc-deficient growth (North *et al.* 2012) and observations by others that autophagy is induced by treatment with a cell-permeable metal chelator (Kawamata *et al.* 2017), we hypothesized that *ATG41* may be required for autophagy induction during zinc deficiency, and that *atg41*Δ mutants grow poorly when zinc-deficient because they are unable to appropriately induce autophagy. To test this hypothesis, we examined autophagic flux using an assay of Ape1 maturation (Klionsky *et al.* 2012). The precursor form of Ape1 (prApe1) is synthesized in the cytosol and delivered to the vacuole constitutively via the cargo-specific cytoplasm-to-vacuole targeting (Cvt) pathway. Vac8 is required for prApe1 to be taken up by the Cvt pathway but is not required for macroautophagy. Therefore, in a *vac8* mutant, prApe1 accumulates in the cytosol and is unable to enter the vacuole. If autophagy is induced, prApe1 is then taken up into autophagosomes nonspecifically and delivered to the vacuole, where it is proteolytically processed to mature Ape1. This processing is detectable by immunoblotting, and the appearance of mature Ape1 in *vac8* cells indicates flux through the autophagy pathway. We grew cells to midlog phase in replete zinc and then shifted them into deficient medium. Protein samples were prepared for immunoblotting at $T = 0$ and after 4 hr. We found that in *vac8* mutant cells, autophagy was induced by zinc deficiency and this induction was reduced in a *vac8*Δ *atg41*Δ double mutant (Figure 3A).

To confirm this phenotype, we performed a second assay using a GFP-Atg8 fusion (Klionsky *et al.* 2012). Atg8 is incorporated into the membranes of phagophores during autophagy and delivered to the vacuole. The Atg8 moiety is then degraded rapidly, but GFP is degraded more slowly, allowing it to accumulate when autophagy is induced. Wild-type cells accumulated free GFP during zinc deficiency but not in replete conditions, confirming that zinc deficiency induces autophagy (Figure 3B). This accumulation was reduced in an *atg41*Δ mutant. An *atg3* mutant, which is completely defective for autophagy, showed no free GFP accumulation. The blot shown is representative of three independent replicates that were quantified (Figure 3C). The observed increase in free GFP abundance between zinc-replete and -deficient wild-type yeast, as well as the decrease in zinc-limited *atg41*Δ yeast, were statistically significant ($P < 0.01$). These data confirmed previous reports that zinc deficiency induces autophagy and also show that *ATG41* is required for the process to be fully induced.

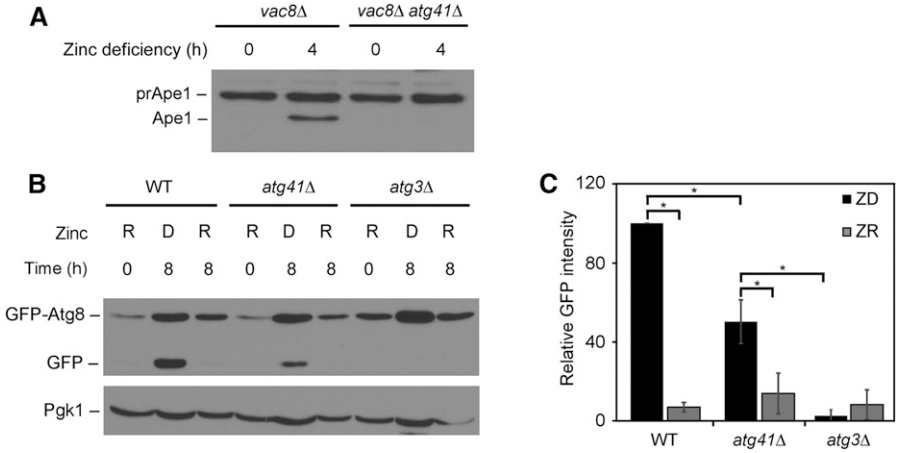

Figure 3 Mutant *atg41*Δ cells are defective for autophagy induced by zinc deficiency. (A) *vac8*Δ and *vac8*Δ *atg41*Δ mutants were grown to midlog phase in zinc-replete medium (ZR) (0 hr), and then transferred to zinc-deficient (ZD) medium for 4 hr. At both time points, samples were collected and used for immunoblotting of Ape1. (B) Wild-type (WT), *atg41*Δ, and *atg3*Δ cells expressing GFP-Atg8 were grown to midlog phase in ZR medium and then transferred to either zinc-replete (R) or zinc-deficient (D) medium for 8 hr. Samples were taken at these time points and used for immunoblotting to detect either GFP or Pgk1 as a loading control. (C) The experiment shown in (B) was performed three times and the quantified GFP band intensities are shown. Error bars represent 1 SD. * $P < 0.01$.

The atg41Δ mutant growth defect is not suppressed by restored autophagy

Our results suggested that *atg41*Δ mutants grow poorly when deficient for zinc due to a failure to fully induce autophagy. However, previous studies had linked *ATG41* to several other processes, including protein homeostasis (Hahn *et al.* 2004; Yeger-Lotem *et al.* 2009) and carbon metabolism (Kuhn *et al.* 2001). These observations raised the possibility that *ATG41* is also required for functions other than autophagy in a zinc-deficient cell. As a test of the ability of restored autophagy to suppress the *atg41*Δ phenotype, we treated wild-type and *atg41*Δ cells with rapamycin. Rapamycin inactivates TORC1 and induces autophagy (Noda and Ohsumi 1998). Wild-type and *atg41*Δ mutant cells were inoculated into a zinc-deficient medium with and without 160 nM rapamycin. After ~40 hr of culturing, we saw no statistically significant suppression of the growth defect (Figure 4A). However, we did confirm, using the GFP-Atg8 assay, that rapamycin treatment induced a very high level of autophagy in both wild-type and *atg41*Δ cells (Figure 4B). Rapamycin induced a much higher level of autophagy than did zinc deficiency. Because the growth defect of *atg41*Δ mutants in zinc-deficient conditions was not suppressed by restored autophagy, we concluded that low autophagy activity was likely not the primary cause of the *atg41*Δ growth defect.

Mutant atg41Δ cells exhibit phenotypes that differ from other autophagy mutant strains

Atg41 was previously shown to physically interact with the Atg9 protein in response to nitrogen starvation (Yao *et al.* 2015). We reasoned that if Atg41's role in autophagy is critical for zinc-deficient growth, disrupting the gene for this binding partner would show a similarly severe phenotype. Atg9 forms a complex with Atg23 and Atg27, so mutations in those genes were tested as well. The *atg9*Δ and *atg23*Δ mutants were slightly defective for zinc-limited growth, but their phenotypes were far less severe than that of the *atg41*Δ mutant (Figure 5A). *atg27*Δ mutants showed no detectable growth defect. We also tested *atg1*Δ and *atg8*Δ mutants, which, like *atg9*Δ mutants, are completely defective for autophagy activity; *atg41*Δ, *atg23*Δ, and *atg27*Δ mutants are only partially defective (Tsukada and Ohsumi 1993; Matsuura *et al.* 1997; Kirisako *et al.* 2000; Yen *et al.* 2007) (Figure 3). Again, *atg41*Δ cells displayed a much more severe zinc-limited growth defect than these other autophagy mutants (Figure 5B). We reasoned that aborted autophagy, caused by the lack of Atg41 function in an *atg41*Δ mutant, might trap the process at a sensitive intermediate stage that disrupts cell growth to a greater degree than the total absence of autophagy. If so, mutations such as *atg1*Δ and *atg8*Δ that block the autophagy process at early steps would be predicted to suppress the *atg41*Δ growth defect. We tested growth of *atg1*Δ *atg41*Δ and *atg8*Δ *atg41*Δ double mutants, but no such suppression was detected (Figure 5B). These results support the hypothesis that the severe growth defect of zinc-deficient *atg41*Δ mutants is due to loss of some autophagy-independent process.

Because of Atg41's previously identified connections to protein homeostasis, we also examined the activity of Hsf1 in zinc-replete and -deficient *atg41*Δ mutants. The Hsf1 transcription factor increases expression of its target genes in response to unfolded protein stress. We first used a reporter plasmid with the Hsf1-responsive *SSA3* promoter driving expression of *lacZ* (Boorstein and Craig 1990). Wild-type and *atg41*Δ mutant cells were grown in zinc-replete and -deficient conditions, and then assayed for β-galactosidase activity. β-galactosidase activity following zinc-replete growth was similarly low for both *atg41*Δ and wild-type cells (Figure 6A). However, in zinc-deficient conditions, *atg41*Δ cells showed ~15-fold higher β-galactosidase activity than in wild-type cells, indicating strong activation of the *SSA3* promoter. To confirm this phenotype, we used a second reporter with a single heat shock element (HSE) inserted upstream of a basal promoter to drive expression of *lacZ* (MacDiarmid *et al.* 2013), and assayed β-galactosidase activity in zinc-replete and deficient wild-type and *atg41*Δ cells. This reporter also showed increased activity specifically in zinc-limited *atg41*Δ mutants (Figure 6B). To test whether the loss of autophagy in

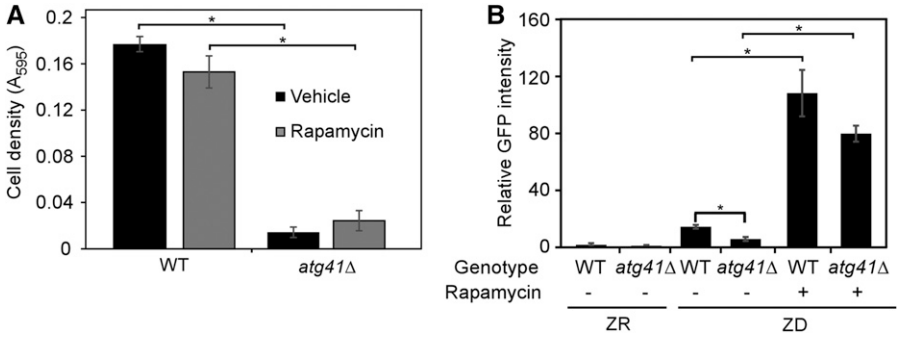

Figure 4 Rapamycin treatment does not rescue the *atg41*Δ zinc-limited growth defect despite inducing autophagy. (A) Wild-type (WT) and *atg41*Δ cells were grown in zinc-deficient medium containing either 160 nM rapamycin or ethanol vehicle. (B) WT and *atg41*Δ cells were grown in zinc-replete medium to midlog phase, sampled, and shifted to zinc-deficient medium containing either 160 nM rapamycin or ethanol vehicle, and grown for an additional 8 hr. Samples were subjected to immunoblotting for GFP as described for Figure 3. Shown are the quantified results of three independent replicates and the error bars represent 1 SD. The asterisks denote $P < 0.01$ by Students *t*-test.

*atg41*Δ mutants is responsible for the observed Hsf1 activity, we assayed HSE-*lacZ* expression in several autophagy mutants (*atg9*Δ, *atg23*Δ, *atg27*Δ, *atg1*Δ, and *atg8*Δ) (Figure 6, B and C). Only *atg41*Δ mutants strongly increased Hsf1 activity in zinc-deficient conditions. These results indicated that Atg41 plays an autophagy-independent role in protein homeostasis when zinc supplies are low.

We also tested the contribution of the paralogous *ICY1* gene to protein homeostasis. While *icy1*Δ mutation alone had no effect on HSE-*lacZ* expression, mutation of *icy1*Δ in an *atg41*Δ mutant further increased HSE-*lacZ* expression during zinc deficiency when compared to the *atg41*Δ single mutant ($P < 0.05$) (Figure 6D). This observation provides additional evidence that Atg41 and Icy1 share one or more autophagy-independent functions in zinc-deficient cells.

*The Met4 transcription factor is activated in zinc-deficient atg41*Δ *cells*

To identify autophagy-independent defects in zinc-deficient *atg41*Δ cells, we performed RNA-seq analysis of mRNA from wild-type and *atg41*Δ cells. Cultures were grown to midlog phase under zinc-replete conditions and then shifted to zinc-deficient medium for 8 hr, after which the cells were harvested for RNA isolation. We chose to harvest cells at that time because it is shortly after *atg41*Δ cells begin to exhibit a detectable growth defect relative to wild-type cells (Figure 7A). Thus, we aimed to identify the proximate transcriptional responses to *atg41*Δ's functional deficits, rather than later indirect responses. Additionally, because it was possible that *atg41*Δ cells would respond to a lack of full autophagy activity (Figure 3), we included an *atg1*Δ strain in the analysis to control for effects on the transcriptome caused by the autophagy defect of the *atg41*Δ mutation. Mutant *atg1*Δ cells showed no detectable growth defect at 8 hr of zinc deficiency (data not shown). RNA-seq data were obtained for ~6100 ORFs for each strain in biological triplicate samples. To quantify gene expression and determine differential expression, we used RSEM and EdgeR, respectively (see *Materials and Methods*). We then calculated false discovery rates to control the prevalence of type-one errors. To designate a gene as differentially expressed between two strains, we required that it be present in the group of genes determined as containing ≤ 5% false positives and show a twofold or greater change to increase the likelihood that expression differences observed were physiologically relevant. These criteria were important because *atg41*Δ mutants, when compared to wild-type (comparison 1) or *atg1*Δ (comparison 2) cells, showed 4229 and 3459 statistically significant differentially expressed genes, respectively. However, most of the changes were small in magnitude (*i.e.*, less than twofold), and only 657 and 702 expression differences were both significant and greater than twofold in magnitude for comparison 1 and comparison 2, respectively. Finally, we focused on differentially expressed genes that were observed in both comparison 1 and comparison 2. Thus, we identified transcriptional changes in *atg41*Δ cells that were likely not due to their autophagy defect. The resulting list comprised 296 downregulated genes and 233 upregulated genes (see Tables S3 and S4 in File S1). Finally, when comparing *atg1*Δ to wild-type cells, we found that the *atg1*Δ mutant expressed only three genes at levels increased by greater than twofold and 11 genes at levels decreased by greater than twofold. These far fewer differences between wild-type and *atg1*Δ cells are consistent with our hypothesis that Atg41 plays an important autophagy-independent role or roles during zinc deficiency.

To identify functionally related groups of genes that were coregulated in zinc-deficient *atg41*Δ mutants, we used GO analysis. Major findings are listed in Tables S5 and S6 in File S1. Genes induced in *atg41*Δ mutants were related to sulfur amino acid metabolism as well as glutamate biosynthesis. Additionally, we observed induction of Ty-elements, which are controlled by many transcription factors and pathways (Errede 1993; Gray and Fassler 1993, 1996; Türkel *et al.* 1997; Dudley *et al.* 1999; Morillon *et al.* 2000; Todeschini *et al.* 2005), and the induction of several hexose transport proteins. We also observed downregulation of ribosomal protein genes and other genes related to translation. These genes are controlled by multiple systems of regulatory factors, and their expression is commonly observed to decrease in response to stress or nutrient limitation, which is expected given the *atg41*Δ mutant growth defect (Gasch *et al.* 2000).

For genes that increase in expression in *atg41*Δ mutants, the GO term with the lowest *P*-value was sulfur amino acid biosynthesis. The sulfur limitation-responsive transcription

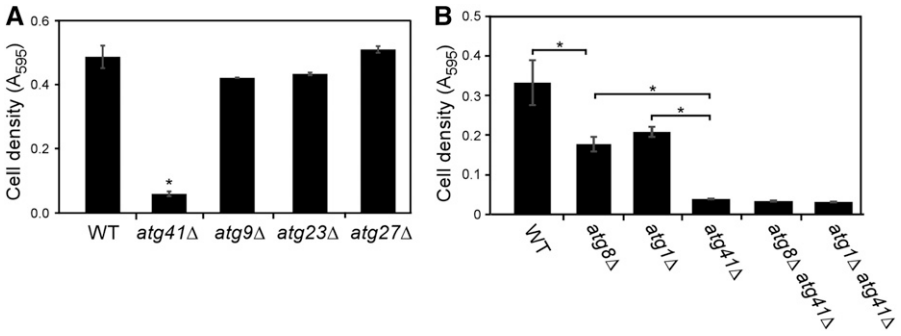

Figure 5 Mutant *atg41*Δ cells exhibit a more severe zinc-limited growth defect than other autophagy gene mutants. For both panels, cells of the indicated genotype were grown in zinc-deficient conditions. Cultures were assayed in triplicate and the error bars represent 1 SD. The asterisks denote $P < 0.01$ (A) or 0.05 (B) by Students *t*-test. WT, wild-type.

factor Met4 controls the expression of genes critical for sulfur metabolism. Through cooperative interaction with DNA-binding proteins, Met4 activates the transcription of ≥ 45 genes in response to sulfur deficiency (Lee *et al.* 2010). Notably, *ATG41* is one of the 45 genes activated by Met4, which is consistent with possible involvement of Atg41 in sulfur metabolism. Among the set of genes whose expression was increased in both comparisons 1 and 2 [false discovery ratio (FDR) < 0.05), 41 out of 44 Met4 target genes appeared and 35 of those increased in expression by more than twofold (Table S7 in File S1).

To confirm the increased expression of Met4 target genes in zinc-deficient *atg41*Δ mutants, and to test whether this phenomenon was zinc-responsive and Met4-dependent, we analyzed the expression of three Met4 target genes—*MET5*, *SUL1*, and *SAM2*—by quantitative RT-PCR in wild-type, *atg1*Δ, and *atg41*Δ cells. We found that only zinc-deficient *atg41*Δ cells showed increased levels of the Met4 target transcripts that we tested (Figure 7B). Moreover, mutation of the *MET4* gene eliminated the response, confirming Met4 dependence (Figure 7C). These results suggest that zinc-deficient *atg41*Δ mutants are somehow disrupted in sulfur metabolism.

Sulfur metabolism is disrupted in zinc-deficient atg41Δ mutants

The culture medium used in these experiments contained two abundant sulfur sources: 40 mM $(NH_4)_2SO_4$ and 670 μM methionine. Additionally, the strains used in these experiments were prototrophic for both cysteine and methionine synthesis. Given these factors, we proposed three possible hypotheses to explain the observed increase in Met4 activity. First, that zinc-deficient *atg41*Δ cells are unable to import either or both sulfur sources from the medium, leading to a *bona fide* sulfur deficiency. Second, that *atg41*Δ cells are defective for the post-translational regulation of Met4 in response to sulfur metabolites. Met4 is regulated by the SCF^{Met30} E3 ubiquitin ligase (Chandrasekaran and Skowyra 2008). Under sulfur-replete conditions, Met4 is ubiquitinated and either inactivated or degraded, and *ATG41* could be required for this regulatory switch to work properly during zinc deficiency. Third, that *atg41*Δ cells are defective for inorganic sulfur assimilation or organic sulfur interconversion, which leads to Met4 activation in response to depletion of a critical form of organic sulfur. Alternatively, one or more sulfur metabolites could be accumulating in an intracellular compartment and thus would be unable to signal sulfur sufficiency.

To address these three hypotheses, we first assayed total sulfur content under zinc-replete and -deficient conditions in wild-type and *atg41*Δ cells. If the first hypothesis was correct, we would expect *atg41*Δ cells to show reduced total sulfur. Wild-type and *atg41*Δ cells were grown in zinc-replete medium and then shifted to the zinc-deficient medium for 4, 8, 12, or 16 hr. At the initial ($T = 0$, zinc replete) and subsequent time points, we collected cells and subjected them to ICP-AES to determine the elemental composition of the samples. As a control for zinc status, we determined zinc content for these cells as well. After 12 hr of growth in zinc-deficient medium, zinc content per milligram of dry mass for both strains decreased by over 10-fold, indicating that they had become zinc-deficient (Figure 8A). However, while no difference was observed for total sulfur accumulation at 0 and 4 hr, we found that at 8, 12, and 16 hr after shifting to zinc-deficient medium, the *atg41*Δ strain had accumulated ∼20% more sulfur per unit mass than wild-type cells ($P < 0.05$). Analysis of other elements—including magnesium, phosphorous, and potassium—showed that the elevated sulfur accumulation was a specific effect (Figure 8A). These results showed that the *atg41*Δ mutants are not experiencing a deficiency in total sulfur. However, these data did not exclude the possibility that *atg41*Δ mutants are defective specifically for methionine uptake, given that cells grown only on SO_4^{2-} have increased Met4 activity (Kuras *et al.* 2002). We found that methionine and $SO4^{2-}$ were equally good sulfur sources for growth of *atg41*Δ cells, indicating that these cells can take up and use methionine during zinc deficiency, with efficacy similar to wild-type (Figure 8B). Thus, these data did not support the hypothesized defect in sulfate or methionine uptake for *atg41*Δ mutants.

To distinguish between dysregulation of Met4 activity and a *bona fide* disruption of sulfur metabolism, we analyzed organic sulfur metabolites in wild-type and *atg41*Δ cells. The hypothesis of dysregulated Met4 activity predicts that the level of at least some sulfur metabolites will increase in zinc-deficient *atg41*Δ mutant cells due to sulfur overaccumulation. Given that low cysteine levels lead to increased Met4 activity (Sadhu *et al.* 2014), cysteine levels should be elevated in zinc-deficient *atg41*Δ mutants if Met4 activity has become uncoupled from sulfur metabolite levels. In contrast,

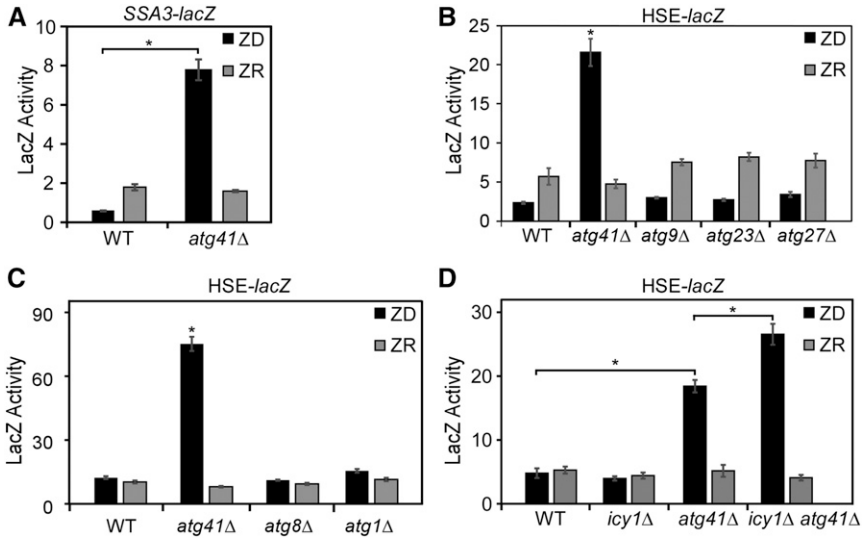

Figure 6 Zinc-deficient *atg41*Δ mutants exhibit increased Hsf1 activity, but other autophagy gene mutants do not. (A) Wild-type (WT) and *atg41*Δ mutants were transformed with pSSA3-LacZ and grown in zinc-replete (ZR) or zinc-deficient (ZD) medium prior to assaying β-galactosidase activity. (B–D) Cells of the indicated genotype were transformed with pHSE-LacZ and grown in ZR or ZD medium prior to assaying β-galactosidase activity. For all panels, LacZ activity was normalized to cell density, cultures were assayed in triplicate, and error bars represent 1 SD. The asterisks denote $P < 0.01$ by Students *t*-test.

if the *atg41*Δ cells are somehow disrupted in their metabolism of sulfur, we predicted that one or more sulfur metabolites would decrease in abundance. A decrease specifically in cysteine level is predicted by this model because of its role in regulating Met4. Wild-type and *atg41*Δ cells were grown to log phase in a zinc-replete medium and then transferred to zinc-deficient conditions for 4, 8, or 12 hr. Cells were collected at each time point and the levels of the sulfur-containing metabolites methionine, homocysteine, cysteine, cystathionine, glutathione, SAM, S-adenosyl homocysteine (SAH), and methylthioadenosine (MTA) were measured in cell lysates by mass spectrometry. The concentrations of these metabolites were normalized to total protein content. In zinc-replete cells, no significant differences were found between wild-type and *atg41*Δ cells (Figure 9). However, after 8 or 12 hr in zinc-limiting medium, the mutant accumulated significantly less methionine, homocysteine, and cysteine ($P < 0.05$). The reduced levels of sulfur metabolites relative to wild-type cells that we observed strongly suggest that sulfur metabolism is indeed disrupted in zinc-deficient *atg41*Δ mutants. Intriguingly, we observed a marked rise in cysteine and homocysteine levels in wild-type cells during the onset of zinc deficiency. These data suggest that wild-type cells respond to zinc deficiency by increasing cysteine levels. When cysteine levels fail to increase in *atg41*Δ cells, Met4 is activated.

Discussion

In this report, we provide the most thorough analysis to date of the importance of Zap1-regulated genes to growth under zinc-deficient conditions. With strains from the yeast deletion collection, we analyzed the growth phenotypes of mutations affecting 66 of the ~80 different Zap1 target genes. Most of the genes that were not tested in this analysis are essential and are therefore not available as null mutant strains. Hypomorphic alleles of many of these essential genes are available and will be examined in future studies. Among the genes tested, *ATG41* was found to be one of the most important for zinc-deficient growth. This growth response is a specific effect, in that *atg41*Δ mutants show no detectable growth defect in zinc-replete cells nor when cells are deficient for other metal nutrients such as copper or iron. Of all Zap1 target genes, the only mutations that cause more severe growth defects are those disrupting *ZRT1*, which encodes the major zinc uptake transporter, and *ZAP1* itself, which is controlled by transcriptional autoregulation. While *ZRT1* and *ZAP1* are required for optimal growth under even mild zinc deficiency, *ATG41* is only needed when severe deficiency occurs. This phenotype is similar to what was previously observed for the Zap1 target genes *TSA1* and *UBI4*, both of which function in the adaptation of cells to the stress of zinc deficiency rather than the maintenance of zinc homeostasis. This observation and our other results are consistent with a role of *ATG41* as another component of the adaptive response to severe zinc deficiency.

Two prior reports have linked *ATG41* to autophagic processes. First, this gene was identified as being required for optimal mitophagy, the cargo-specific degradation of mitochondria (Kanki *et al.* 2009). More recently, *ATG41* was shown to be required for optimal autophagy in response to nitrogen starvation. Experiments that we conducted to assess mitophagy during zinc deficiency detected no mitophagy activity, even in wild-type cells (data not shown). However, assays of autophagy showed that strong induction of this process did occur in zinc-deficient cells. This observation is consistent with the prior work of Carman and colleagues, who detected lipidation of Atg8 during zinc deficiency. Attachment of phosphotidylethanolamine to Atg8 is a key step in autophagosome formation. Our observations also confirm the conclusion of Ohsumi and colleagues that zinc deficiency induced autophagic flux. This latter study was performed using a cell-permeable chelator that perturbs intracellular zinc levels and can strip the metal from zinc-binding proteins. Here, we show that autophagy is induced by nutritional zinc

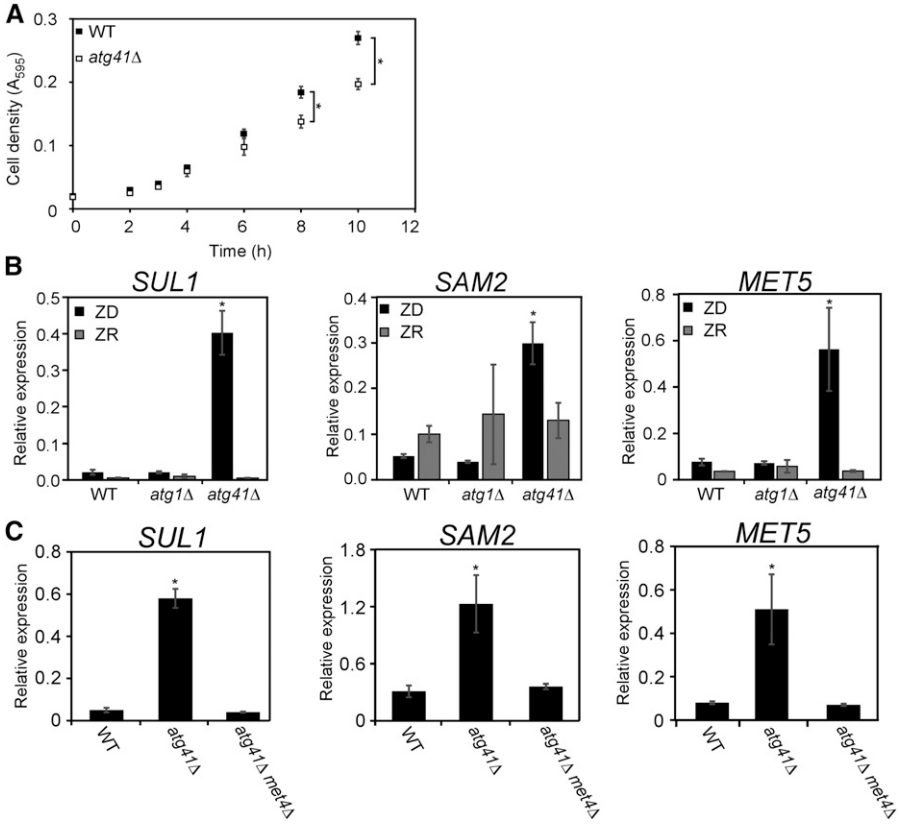

Figure 7 Zinc-deficient *atg41*Δ mutants exhibit increased Met4 activity. (A) Wild-type (WT) and *atg41*Δ mutants were grown to midlog phase in zinc-replete (ZR) medium, and then transferred to zinc-deficient (ZD) medium. The optical densities of the cultures were taken periodically to determine when the mutant strain began to grow differently from WT cells. (B) WT, *atg1*Δ, and *atg41*Δ mutants were grown to midlog phase in ZR medium and then transferred to ZD medium for 8 hr. Quantitative RT-PCR analysis was performed on the resulting samples to quantify expression of the indicated mRNAs. (C) WT, *atg41*Δ, and *atg41*Δ *met4*Δ mutants were grown to midlog phase in ZR medium and then transferred to ZD medium for 8 hr. Quantitative RT-PCR analysis was performed on the resulting zinc-limited samples to quantify expression of the indicated mRNAs. For all panels, cultures were assayed in triplicate and error bars represent 1 SD. The asterisks denote $P < 0.05$ by Students *t*-test.

deficiency and is not an artifact of chelator treatment. The functional importance of induced autophagy during zinc deficiency is not yet clear, but an attractive hypothesis is that this system allows for the recycling of bound zinc atoms for use by newly synthesized zinc proteins (Kawamata *et al.* 2017). This would allow for a limited supply of zinc to be redistributed to sites of higher priority for zinc-deficient growth. Ohsumi and colleagues (Kawamata *et al.* 2017) showed that autophagy was induced normally in zinc-deficient *zap1*Δ mutant cells. These results suggest that the basal level of Atg41 expressed in *zap1*Δ mutant cells is sufficient to mediate normal autophagy in zinc-deficient cells. Given this result, we speculate that the induction of *ATG41* by Zap1 may be to facilitate its autophagy-independent function(s) rather than autophagy.

As was observed during nitrogen starvation, *ATG41* is required for full autophagic flux under zinc-deficient conditions. However, we offer several lines of evidence indicating that the importance of *ATG41* function to growth during zinc deficiency is not because of its role in autophagy, but rather is due to its function in one or more autophagy-independent processes. For example, inducing autophagy with rapamycin failed to improve growth of *atg41*Δ mutants in limiting zinc. In addition, *atg41*Δ mutants show a far more severe growth defect than any of the other autophagy mutants tested, despite the fact that many of these other mutations completely block the process while the *atg41*Δ mutation causes only a partial block. Similarly, *atg41*Δ mutants showed increased Hsf1 activity while other autophagy mutants did not. An autophagy-independent function for *ATG41* in sulfur metabolism during zinc deficiency was identified in our analysis of the transcriptome of *atg41*Δ mutants relative to wild-type cells and autophagy-defective *atg1*Δ mutants during the transition from zinc-replete to deficient conditions. This analysis detected a strong and very specific effect on the activity of the Met4 transcription factor that was not connected to an autophagy defect; no such effect was observed in the *atg1*Δ mutant. Because this response occurred very early in the transition and around the time that the growth defect first becomes apparent, we suggest that this activity is a proximal response to the absence of Atg41 function and not due to later, more indirect effects. Met4 activity increases in response to low-sulfur conditions, so increased Met4 activity was unexpected given the abundant sulfate and methionine in the medium. We proposed three hypotheses to explain the results: (1) defective sulfate and/or methionine uptake, (2) dysregulation of Met4 activity, and (3) disruption of sulfur assimilation or interconversion. The third hypothesis of disrupted sulfur metabolism was supported by our analysis of sulfur metabolites; *atg41*Δ mutants accumulate lower-than-normal levels of cysteine, homocysteine, and methionine than do zinc-deficient wild-type cells. With the observation that total sulfur levels rise in *atg41*Δ mutants, we propose that the disruption in sulfur metabolism caused by *atg41*Δ mutation leads to accumulation of one or more sulfur-containing metabolites not measured in our assays. For example, disruption of glutathione synthesis or degradation could lead to the accumulation of L-γ-glutamylcysteine or L-cysteinylglycine, respectively.

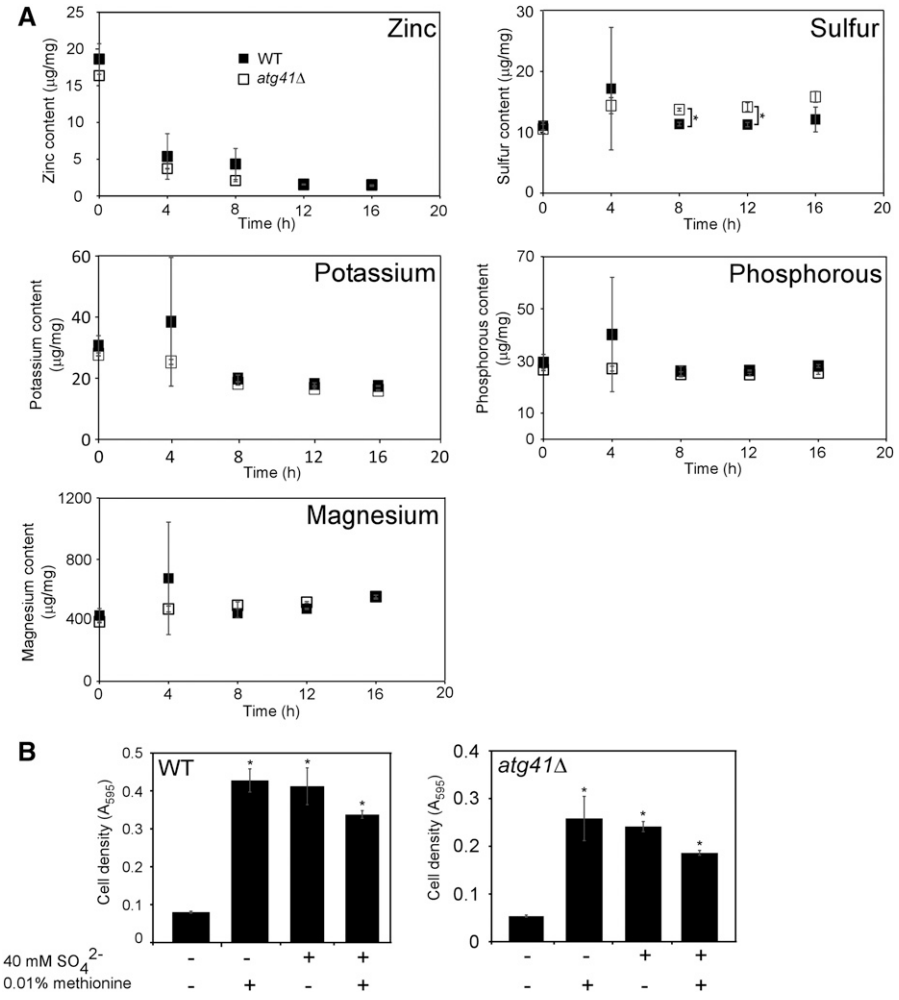

Figure 8 Zinc-deficient *atg41*Δ mutants accumulate more total sulfur than wild-type (WT) cells. (A) WT cells (filled squares) and *atg41*Δ mutants (open squares) were grown to midlog phase in zinc-replete medium ($T = 0$) and then transferred to zinc-deficient medium. Cells were sampled at 4-hr intervals for analysis by inductively coupled plasma atomic emission spectrometry. Data for zinc, sulfur, potassium, phosphorus, and magnesium are plotted normalized to dry mass of the cell pellet. (B) WT and *atg41*Δ mutant cells were grown in zinc-deficient, low-sulfur limited zinc medium supplemented with 40 mM $(NH_4)_2SO_4$, 670 μM methionine, or both. For all panels, cultures were assayed in triplicate and error bars represent 1 SD. The asterisks denote $P < 0.01$ by Students *t*-test.

Given that glutathione is synthesized from cysteine, the lack of an effect of *atg41*Δ mutation on total glutathione levels was unexpected given the marked decrease in cysteine levels. However, these results are consistent with previous studies showing that two zinc-dependent transcription factors, Nil1 and Gln3, activate expression of the *CIS2* gene (Springael and Penninckx 2003). Cis2 is one of two sequentially acting glutathione-degrading enzymes. These transcription factors may be less active in zinc-deficient cells, thereby leading to decreased *CIS2* expression and slower glutathione degradation. In addition, the second enzyme in the pathway is Dug1, which is zinc-dependent for its catalytic function (Kaur *et al.* 2009). Decreased Dug1 activity resulting from zinc deficiency could also cause impaired glutathione degradation.

A close analysis of the sulfur metabolites revealed a particularly interesting effect of zinc deficiency on sulfur metabolism and its regulation in wild-type cells. First, the levels of key metabolites homocysteine and cysteine increased twofold and fourfold, respectively, in zinc-deficient wild-type cells. One explanation for this effect is that zinc deficiency reduces the activity of the zinc-dependent Met6 methionine synthetase enzyme due to the scarcity of its required cofactor. Met6 methylates homocysteine to form methionine and its decreased activity could increase homocysteine and, indirectly, cysteine levels, which are generated through the intermediate cystathionine. Alternatively, the increase in homocysteine and cysteine levels could indicate a change in the set point of regulation for sulfur metabolism. The level of cysteine in cells is thought to be a key signal of sulfur status that controls Met4 activity (Sadhu *et al.* 2014). While the mechanism of cysteine sensing that controls Met4 activity has not been clearly defined, an altered set point of Met4 regulation could also explain the increase in cysteine accumulation in zinc-deficient wild-type cells. Evidence for an altered set point is in fact observed in the results from the *atg41*Δ mutant. While cysteine levels do not rise to the high level observed in wild-type cells, they do increase by around twofold relative to zinc-replete cells. Whereas the level of cysteine in zinc-replete cells is sufficient to repress Met4 activity, the even higher levels of cysteine in zinc-deficient *atg41*Δ cells are not. Thus, the set point for Met4 regulation does indeed appear to be altered by zinc status. Whatever the mechanism, the increase in cysteine in zinc-deficient wild-type cells may be of functional importance to growth under these conditions. Cysteine has been proposed to be an intracellular facilitator of metallation

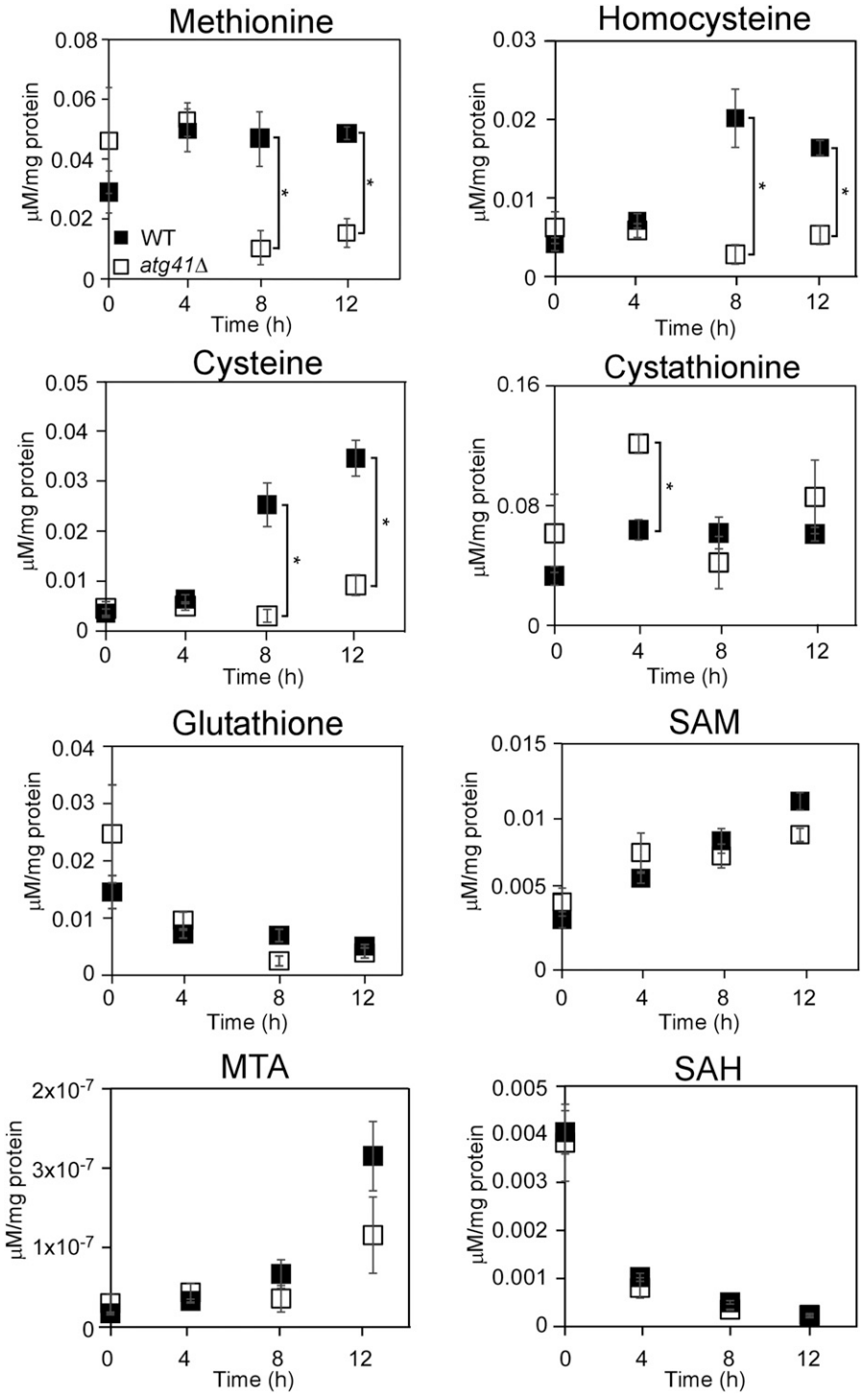

Figure 9 Zinc-deficient *atg41*Δ mutants show lower accumulation of key sulfur metabolites. Wild-type (WT) (filled squares) and *atg41*Δ mutant (open squares) cells were grown to midlog phase in zinc-replete medium ($T = 0$), and then transferred to zinc-deficient medium for 12 hr. Cells were harvested at 4-hr intervals for metabolite analysis by LC-MS/MS. Metabolite concentration values were normalized to total protein. For all panels, cultures were assayed in triplicate and error bars represent 1 SD. The asterisks denote $P < 0.01$ by Students *t*-test. MTA, methylthioadenosine; SAH, S-adenosyl homocysteine; SAM, S-adenosyl methionine.

reactions (Gu and Imlay 2013). Zinc can bind to other nonfunctional sites within the cell, and the elevated cysteine could aid in extraction of that zinc so that it can be bound more stably by zinc metalloproteins.

It is tempting to speculate that the severe growth defect of *atg41*Δ mutants during zinc deficiency is caused by the disruption of sulfur metabolism. We have attempted to establish this link experimentally but no connection has yet been made. For example, one hypothesis is that *atg41*Δ mutants grow poorly because the levels of sulfur metabolites such as cysteine and/or homocysteine need to rise to the levels observed in wild-type cells. This hypothesis predicts that supplements of cysteine and/or homocysteine added to the medium would improve growth of zinc-deficient *atg41*Δ mutants. We have performed those experiments and no benefit to growth was observed (Figure S3 in File S1). A second hypothesis is that sulfur accumulates in *atg41*Δ mutants in a form that is toxic to these cells. This hypothesis predicts that

reduced levels of sulfur in the medium might lower the level of this toxic metabolite and thereby rescue growth. Reducing levels of sulfate and/or methionine in the medium had no effect on the growth of zinc-deficient *atg41*Δ mutants until the point when those levels became insufficient for even the poor growth of these cells (Figure S4 in File S1). A third hypothesis stems from the observation that overexpressed Met4 activity causes an arrest in the cell cycle (Patton *et al.* 2000). This arrest is suppressed by mutations in *MET4* and also by mutations in the *MET32* gene encoding a DNA-binding accessory protein required for Met4-activated transcription. Neither mutation suppressed the *atg41*Δ growth defect in zinc deficiency (data not shown). Thus, it is unclear whether the growth defect in zinc-deficient cells is a result of disrupted sulfur metabolism or an as yet undiscovered additional function of Atg41.

Atg41 is likely to play a role in the response to a number of stress conditions because its gene is regulated by several stress-responsive transcription factors, *i.e.*, Zap1 (zinc deficiency), Met4 (sulfur deficiency), Gcn4 (nitrogen starvation), and Hsf1 (protein misfolding). Moreover, translation of *ATG41* mRNA is regulated in response to carbon source. The role of Atg41 in autophagy and its autophagy-independent function in zinc-deficient cells suggests that Atg41 is a multifunctional protein. Given the amino acid sequence of this protein, this is a surprising conclusion. Atg41 is a small, highly acidic protein with little predicted secondary structure and no conserved domains. Atg41 does contain large regions that are predicted to be intrinsically disordered. It is this observation that suggests a possible function for Atg41 that could apply to autophagy, sulfur metabolism, and perhaps other functions. Intrinsically disordered proteins such as SNCA/α-synuclein, CALD1/caldesmon 1, HMGA, and VAMP/synaptobrevin are increasingly recognized as "hub" proteins that can mediate the formation of protein interaction networks (Dunker *et al.* 2005). In the case of autophagy, Atg41 interacts with the Atg9 protein, which also interacts with at least two additional factors, Atg23 and Atg27. It is therefore conceivable that Atg41 serves to coordinate the assembly of this complex. Similarly, enzyme complexes may form in sulfur metabolism and the efficiency of their function could also rely on complex assembly mediated by Atg41. We are currently assessing this model by co-immunoprecipitation and mass spectrometry analysis, but the low abundance of Atg41 protein renders this a challenging experiment.

Finally, our phenotypic analysis of Zap1-regulated genes has greatly expanded the list of these genes with proven effects on growth during zinc deficiency. Most of the mutations with effects on growth broke down into two groups: mutants that grew less well than wild-type cells when zinc-deficient and those that grew better. Given that the primary function of Zap1 is to activate gene expression during zinc deficiency, this latter group (13 of 66 tested) was unexpected. However, we can explain this paradoxical phenotype for the *zrt3*Δ mutant. The Zrt3 zinc transporter is responsible for moving stored zinc out of the vacuole into the cytosol for utilization. While it is induced during zinc deficiency, this protein is expressed in zinc-replete cells. *zrt3*Δ mutants grown in zinc-replete conditions hyperaccumulate vacuolar zinc relative to wild-type cells (MacDiarmid *et al.* 2000). In our growth experiments, cells were initially grown in zinc-replete conditions prior to inoculation into the zinc-deficient medium so the extra zinc stores in the *zrt3*Δ mutant could be mobilized by other, as yet unknown transporters for use and give a growth advantage to this mutant strain. Conversely, we now have identified 31 of the Zap1 target genes that are required for optimal growth under zinc deficiency, *i.e.*, a large increase from the nine genes previously identified as having a growth defect. While many of these effects are mild, the fact that we can detect them after only 15 generations indicates that they would be relevant over longer timescales of natural selection. These genes play diverse roles in zinc homeostasis, protein homeostasis, oxidative stress resistance, lipid metabolism, gene expression, and cell wall function, and, as we now recognize for *ATG41*, autophagy and sulfur metabolism.

Acknowledgments

The authors thank Colin MacDiarmid for expert advice and assistance throughout this project. This work was supported by National Institutes of Health grants RO1 GM-056285 to D.J.E., and P41 GM-108538 and R35 GM-118110 to J.C. We also acknowledge support from the Morgridge Institute of Research Metabolism Theme and the Laboratory of Biomolecular Mass Spectrometry.

Literature Cited

Boorstein, W. R., and E. A. Craig, 1990 Transcriptional regulation of SSA3, an HSP70 gene from Saccharomyces cerevisiae. Mol. Cell. Biol. 10: 3262–3267.

Chandrasekaran, S., and D. Skowyra, 2008 The emerging regulatory potential of SCFMet30 -mediated polyubiquitination and proteolysis of the Met4 transcriptional activator. Cell Div. 3: 11.

De Nicola, R., L. A. Hazelwood, E. A. De Hulster, M. C. Walsh, T. A. Knijnenburg *et al.*, 2007 Physiological and transcriptional responses of Saccharomyces cerevisiae to zinc limitation in chemostat cultures. Appl. Environ. Microbiol. 73: 7680–7692.

Dobin, A., C. A. Davis, F. Schlesinger, J. Drenkow, C. Zaleski *et al.*, 2013 STAR: ultrafast universal RNA-seq aligner. Bioinformatics 29: 15–21.

Dudley, A. M., L. J. Gansheroff, and F. Winston, 1999 Specific components of the SAGA complex are required for Gcn4- and Gcr1-mediated activation of the his4–912delta promoter in Saccharomyces cerevisiae. Genetics 151: 1365–1378.

Dunker, A. K., M. S. Cortese, P. Romero, L. M. Iakoucheva, and V. N. Uversky, 2005 Flexible nets. The roles of intrinsic disorder in protein interaction networks. FEBS J. 272: 5129–5148.

Errede, B., 1993 MCM1 binds to a transcriptional control element in Ty1. Mol. Cell. Biol. 13: 57–62.

Gasch, A. P., P. T. Spellman, C. M. Kao, O. Carmel-Harel, M. B. Eisen *et al.*, 2000 Genomic expression programs in the response of yeast cells to environmental changes. Mol. Biol. Cell 11: 4241–4257.

Gietz, D., A. St Jean, R. A. Woods, and R. H. Schiestl, 1992 Improved method for high efficiency transformation of intact yeast cells. Nucleic Acids Res. 20: 1425.

Gray, W. M., and J. S. Fassler, 1993 Role of Saccharomyces cerevisiae Rap1 protein in Ty1 and Ty1-mediated transcription. Gene Expr. 3: 237–251.
Gray, W. M., and J. S. Fassler, 1996 Isolation and analysis of the yeast TEA1 gene, which encodes a zinc cluster Ty enhancer-binding protein. Mol. Cell. Biol. 16: 347–358.
Gu, M., and J. A. Imlay, 2013 Superoxide poisons mononuclear iron enzymes by causing mismetallation. Mol. Microbiol. 89: 123–134.
Guarente, L., 1983 Yeast promoters and lacZ fusions designed to study expression of cloned genes in yeast. Methods Enzymol. 101: 181–191.
Hahn, J. S., Z. Hu, D. J. Thiele, and V. R. Iyer, 2004 Genome-wide analysis of the biology of stress responses through heat shock transcription factor. Mol. Cell. Biol. 24: 5249–5256.
Han, S. H., G. S. Han, W. M. Iwanyshyn, and G. M. Carman, 2005 Regulation of the PIS1-encoded phosphatidylinositol synthase in Saccharomyces cerevisiae by zinc. J. Biol. Chem. 280: 29017–29024.
Hanscho, M., D. E. Ruckerbauer, N. Chauhan, H. F. Hofbauer, S. Krahulec *et al.*, 2012 Nutritional requirements of the BY series of Saccharomyces cerevisiae strains for optimum growth. FEMS Yeast Res. 12: 796–808.
Iwanyshyn, W. M., G. S. Han, and G. M. Carman, 2004 Regulation of phospholipid synthesis in Saccharomyces cerevisiae by zinc. J. Biol. Chem. 279: 21976–21983.
Jiang, H., R. Lei, S. W. Ding, and S. Zhu, 2014 Skewer: a fast and accurate adapter trimmer for next-generation sequencing paired-end reads. BMC Bioinformatics 15: 182.
Kanki, T., K. Wang, M. Baba, C. R. Bartholomew, M. A. Lynch-Day *et al.*, 2009 A genomic screen for yeast mutants defective in selective mitochondria autophagy. Mol. Biol. Cell 20: 4730–4738.
Kaur, H., C. Kumar, C. Junot, M. B. Toledano, and A. K. Bachhawat, 2009 Dug1p is a Cys-Gly peptidase of the gamma-glutamyl cycle of Saccharomyces cerevisiae and represents a novel family of Cys-Gly peptidases. J. Biol. Chem. 284: 14493–14502.
Kawamata, T., T. Horie, M. Matsunami, M. Sasaki, and Y. Ohsumi, 2017 Zinc starvation induces autophagy in yeast. J. Biol. Chem. 292: 8520–8530.
Kersting, M. C., and G. M. Carman, 2006 Regulation of the Saccharomyces cerevisiae EKI1-encoded ethanolamine kinase by zinc depletion. J. Biol. Chem. 281: 13110–13116.
Kirisako, T., Y. Ichimura, H. Okada, Y. Kabeya, N. Mizushima *et al.*, 2000 The reversible modification regulates the membrane-binding state of Apg8/Aut7 essential for autophagy and the cytoplasm to vacuole targeting pathway. J. Cell Biol. 151: 263–276.
Klionsky, D. J., F. C. Abdalla, H. Abeliovich, R. T. Abraham, A. Acevedo-Arozena *et al.*, 2012 Guidelines for the use and interpretation of assays for monitoring autophagy. Autophagy 8: 445–544.
Kraft, C., F. Reggiori, and M. Peter, 2009 Selective types of autophagy in yeast. Biochim. Biophys. Acta 1793: 1404–1412.
Kuhn, K. M., J. L. DeRisi, P. O. Brown, and P. Sarnow, 2001 Global and specific translational regulation in the genomic response of Saccharomyces cerevisiae to a rapid transfer from a fermentable to a nonfermentable carbon source. Mol. Cell. Biol. 21: 916–927.
Kuras, L., A. Rouillon, T. Lee, R. Barbey, M. Tyers *et al.*, 2002 Dual regulation of the met4 transcription factor by ubiquitin-dependent degradation and inhibition of promoter recruitment. Mol. Cell 10: 69–80.
Lee, T. A., P. Jorgensen, A. L. Bognar, C. Peyraud, D. Thomas *et al.*, 2010 Dissection of combinatorial control by the Met4 transcriptional complex. Mol. Biol. Cell 21: 456–469.
Li, B., and C. N. Dewey, 2011 RSEM: accurate transcript quantification from RNA-Seq data with or without a reference genome. BMC Bioinformatics 12: 323.
Lyons, T. J., A. P. Gasch, L. A. Gaither, D. Botstein, P. O. Brown *et al.*, 2000 Genome-wide characterization of the Zap1p zinc-responsive regulon in yeast. Proc. Natl. Acad. Sci. USA 97: 7957–7962.
MacDiarmid, C. W., L. A. Gaither, and D. Eide, 2000 Zinc transporters that regulate vacuolar zinc storage in Saccharomyces cerevisiae. EMBO J. 19: 2845–2855.
MacDiarmid, C. W., J. Taggart, K. Kerdsomboon, M. Kubisiak, S. Panascharoen *et al.*, 2013 Peroxiredoxin chaperone activity is critical for protein homeostasis in zinc-deficient yeast. J. Biol. Chem. 288: 31313–31327.
MacDiarmid, C. W., J. Taggart, J. Jeong, K. Kerdsomboon, and D. J. Eide, 2016 Activation of the yeast UBI4 polyubiquitin gene by Zap1 transcription factor via an intragenic promoter is critical for zinc-deficient growth. J. Biol. Chem. 291: 18880–18896.
Matsuura, A., M. Tsukada, Y. Wada, and Y. Ohsumi, 1997 Apg1p, a novel protein kinase required for the autophagic process in Saccharomyces cerevisiae. Gene 192: 245–250.
Morillon, A., M. Springer, and P. Lesage, 2000 Activation of the Kss1 invasive-filamentous growth pathway induces Ty1 transcription and retrotransposition in Saccharomyces cerevisiae. Mol. Cell. Biol. 20: 5766–5776.
Noda, T., and Y. Ohsumi, 1998 Tor, a phosphatidylinositol kinase homologue, controls autophagy in yeast. J. Biol. Chem. 273: 3963–3966.
North, M., J. Steffen, A. V. Loguinov, G. R. Zimmerman, C. D. Vulpe *et al.*, 2012 Genome-wide functional profiling identifies genes and processes important for zinc-limited growth of Saccharomyces cerevisiae. PLoS Genet. 8: e1002699.
Outeiro, T. F., and S. Lindquist, 2003 Yeast cells provide insight into alpha-synuclein biology and pathobiology. Science 302: 1772–1775.
Patton, E. E., C. Peyraud, A. Rouillon, Y. Surdin-Kerjan, M. Tyers *et al.*, 2000 SCF(Met30)-mediated control of the transcriptional activator Met4 is required for the G(1)-S transition. EMBO J. 19: 1613–1624.
Robinson, M. D., D. J. McCarthy, and G. K. Smyth, 2010 edgeR: a bioconductor package for differential expression analysis of digital gene expression data. Bioinformatics 26: 139–140.
Sadhu, M. J., J. J. Moresco, A. D. Zimmer, J. R. Yates, III, and J. Rine, 2014 Multiple inputs control sulfur-containing amino acid synthesis in Saccharomyces cerevisiae. Mol. Biol. Cell 25: 1653–1665.
Singh, N., K. K. Yadav, and R. Rajasekharan, 2016 ZAP1-mediated modulation of triacylglycerol levels in yeast by transcriptional control of mitochondrial fatty acid biosynthesis. Mol. Microbiol. 100: 55–75.
Soto, A., and G. M. Carman, 2008 Regulation of the Saccharomyces cerevisiae CKI1-encoded choline kinase by zinc depletion. J. Biol. Chem. 283: 10079–10088.
Soto-Cardalda, A., S. Fakas, F. Pascual, H. S. Choi, and G. M. Carman, 2012 Phosphatidate phosphatase plays role in zinc-mediated regulation of phospholipid synthesis in yeast. J. Biol. Chem. 287: 968–977.
Spiess, C., A. S. Meyer, S. Reissmann, and J. Frydman, 2004 Mechanism of the eukaryotic chaperonin: protein folding in the chamber of secrets. Trends Cell Biol. 14: 598–604.
Springael, J. Y., and M. J. Penninckx, 2003 Nitrogen-source regulation of yeast gamma-glutamyl transpeptidase synthesis involves the regulatory network including the GATA zinc-finger factors Gln3, Nil1/Gat1 and Gzf3. Biochem. J. 371: 589–595.
Stephan, J. S., Y. Y. Yeh, V. Ramachandran, S. J. Deminoff, and P. K. Herman, 2009 The Tor and PKA signaling pathways independently target the Atg1/Atg13 protein kinase complex to control autophagy. Proc. Natl. Acad. Sci. USA 106: 17049–17054.

Sutter, B. M., X. Wu, S. Laxman, and B. P. Tu, 2013 Methionine inhibits autophagy and promotes growth by inducing the SAM-responsive methylation of PP2A. Cell 154: 403–415.

Suzuki, K., T. Kirisako, Y. Kamada, N. Mizushima, T. Noda *et al.*, 2001 The pre-autophagosomal structure organized by concerted functions of APG genes is essential for autophagosome formation. EMBO J. 20: 5971–5981.

Suzuki, K., Y. Kubota, T. Sekito, and Y. Ohsumi, 2007 Hierarchy of Atg proteins in pre-autophagosomal structure organization. Genes Cells 12: 209–218.

Todeschini, A. L., A. Morillon, M. Springer, and P. Lesage, 2005 Severe adenine starvation activates Ty1 transcription and retrotransposition in Saccharomyces cerevisiae. Mol. Cell. Biol. 25: 7459–7472.

Tsukada, M., and Y. Ohsumi, 1993 Isolation and characterization of autophagy-defective mutants of Saccharomyces cerevisiae. FEBS Lett. 333: 169–174.

Türkel, S., X. B. Liao, and P. J. Farabaugh, 1997 GCR1-dependent transcriptional activation of yeast retrotransposon Ty2-917. Yeast 13: 917–930.

Wu, C. Y., A. J. Bird, L. M. Chung, M. A. Newton, D. R. Winge *et al.*, 2008 Differential control of Zap1-regulated genes in response to zinc deficiency in Saccharomyces cerevisiae. BMC Genomics 9: 370.

Wu, C. Y., S. Roje, F. J. Sandoval, A. J. Bird, D. R. Winge *et al.*, 2009 Repression of sulfate assimilation is an adaptive response of yeast to the oxidative stress of zinc deficiency. J. Biol. Chem. 284: 27544–27556.

Wu, X., and B. P. Tu, 2011 Selective regulation of autophagy by the Iml1-Npr2-Npr3 complex in the absence of nitrogen starvation. Mol. Biol. Cell 22: 4124–4133.

Yao, Z., E. Delorme-Axford, S. K. Backues, and D. J. Klionsky, 2015 Atg41/Icy2 regulates autophagosome formation. Autophagy 11: 2288–2299.

Yeger-Lotem, E., L. Riva, L. J. Su, A. D. Gitler, A. G. Cashikar *et al.*, 2009 Bridging high-throughput genetic and transcriptional data reveals cellular responses to alpha-synuclein toxicity. Nat. Genet. 41: 316–323.

Yen, W. L., J. E. Legakis, U. Nair, and D. J. Klionsky, 2007 Atg27 is required for autophagy-dependent cycling of Atg9. Mol. Biol. Cell 18: 581–593.

Yin, Z., C. Pascual, and D. J. Klionsky, 2016 Autophagy: machinery and regulation. Microb. Cell 3: 588–596.

Zhao, H., and D. Eide, 1996 The yeast ZRT1 gene encodes the zinc transporter protein of a high-affinity uptake system induced by zinc limitation. Proc. Natl. Acad. Sci. USA 93: 2454–2458.

Communicating editor: D. Lew